Supplementary Figure 1. Transcriptome analysis of genes with consistent expression in response to drought and *Fusarium pseudograminearum* (*Fpg*) infection. (a) Differentially expressed genes (DEGs) up-regulated in response to drought and *Fpg* infection. (b) DEGs down-regulated in response to drought and *Fpg* infection. (c) Gene ontology (GO) enrichment analysis of DEGs with consistent expression in response to drought and *Fpg* infection. BP, Biological Process; CC, Cell Component; MF, Molecular Function.

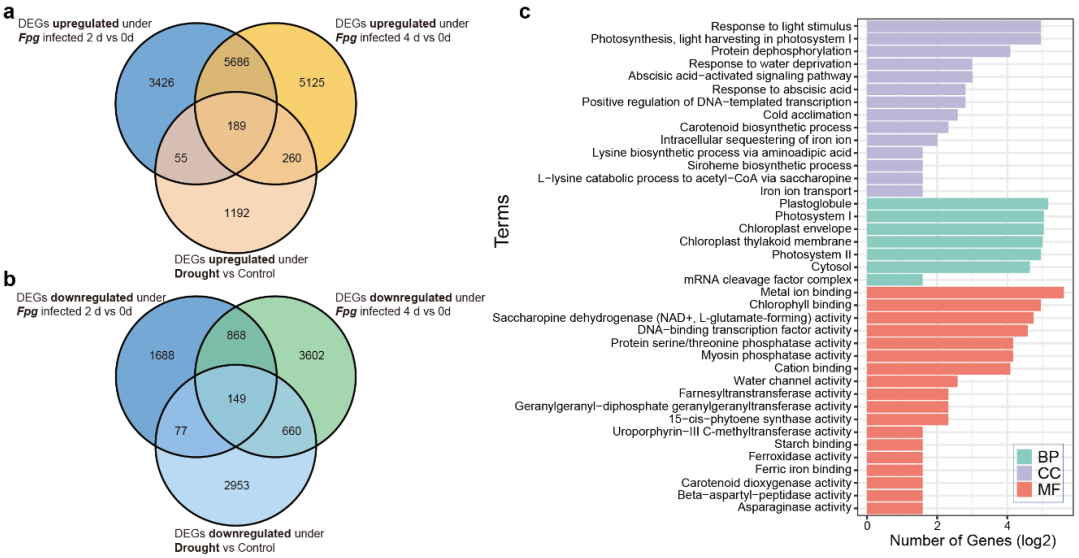

Supplementary Figure 2. GO enrichment analysis of 762 DEGs up-regulated under *Fpg* infection and down-regulated in response to drought treatment. BP, Biological Process; CC, Cell Component; MF, Molecular Function.

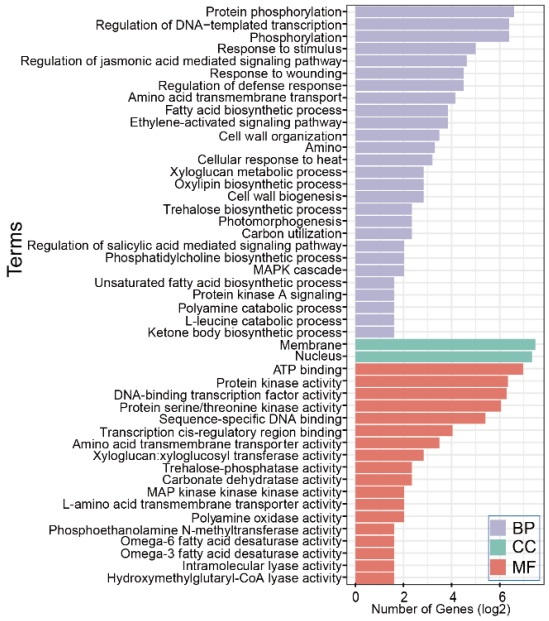

Supplementary Figure 3. The expression pattern and protein abundance of the *TaMPK3* genes. (a-b) Expression of *TaMPK3* genes in key cultivated varieties were analyzed under drought and FCR stress. In box plots, the line represents the median, the edges of the box define the interquartile range, and the whiskers represent the minimum and maximum values. (c) The protein abundance of TaMPK3 was quantified following infection with *Fpg*. Statistical significance was determined by a two-tailed Student's t test (*p < 0.05, **p < 0.01, ***p < 0.001).

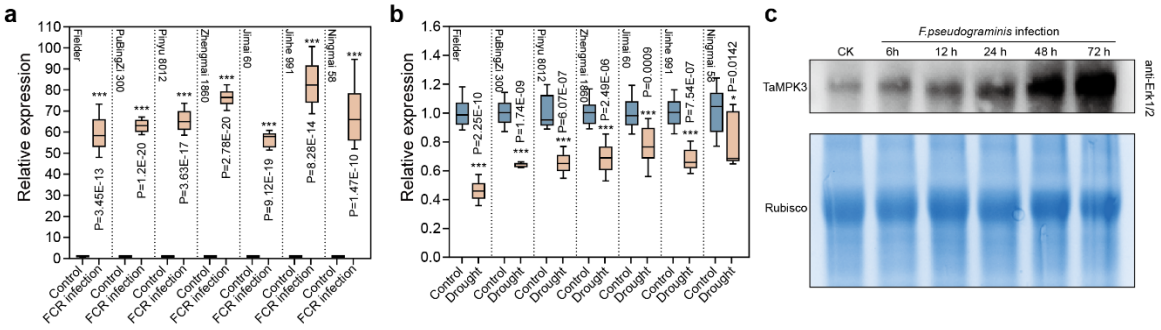

Supplementary Figure 4. Tissue expression pattern and protein sequence analysis of the *TaMPK3* genes. (a) Expression level of *TaMPK3* genes in different tissues and growth stages. Data are presented as mean values +/- SD. (b) The amino acid sequences of TaMPK3 proteins exhibited 99.91% identity among their homologues. The protein sequence of kinase domains is shown in yellow. The red box indicates the differential amino acid sites in the TaMPK3 homologous protein.

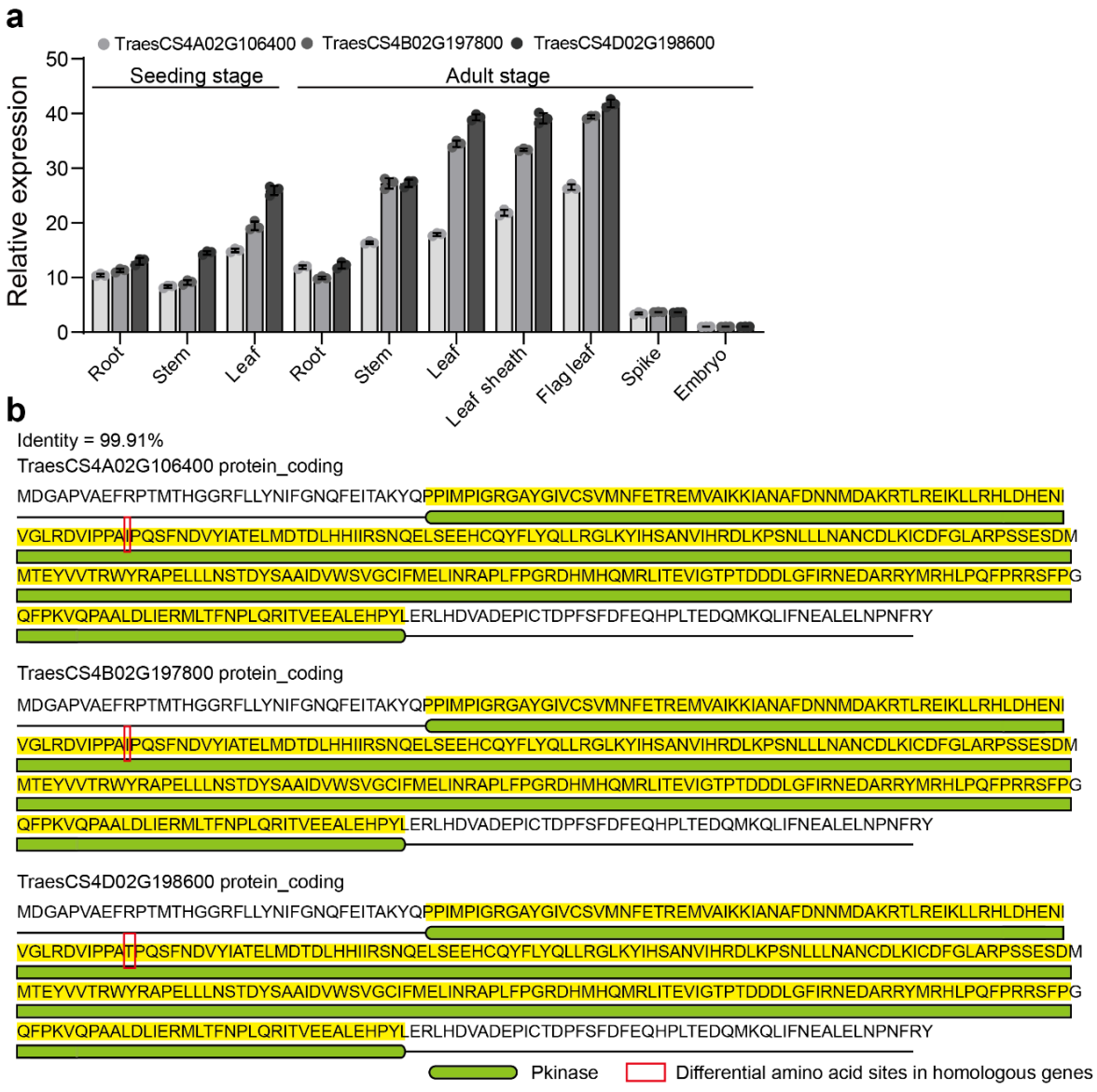

Supplementary Figure 5. Frameshift mutations and premature stop codons caused by genomic variations in chromosomes A, B, and D in the gene-edited *TaMPK3*-KO lines. The kinase domain protein sequences are highlighted in yellow; the frameshift mutation induced by gene editing is indicated in red; and the truncated protein sequence resulting from premature termination codons is displayed in black.

Supplementary Figure 6. Analysis of TaMPK3 protein abundance in transgenic lines (*TaMPK3*-OE and *TaMPK3*-KO) and wild-type (WT) plants.

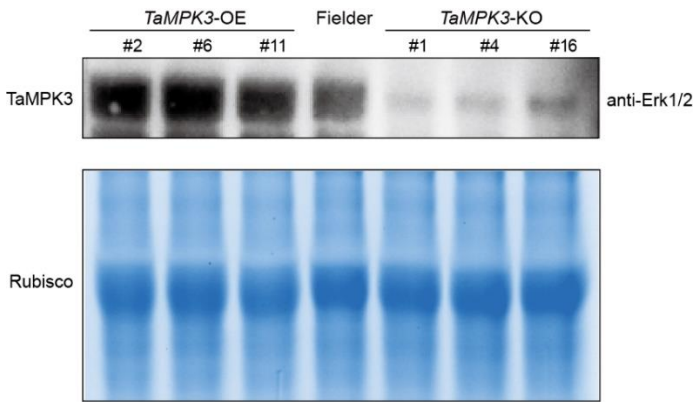

Supplementary Figure 7. The grain traits were analyzed in transgenic lines and WT plants. (a-b) The grain traits of transgenic lines and WT plants under normal and drought conditions in the field; bars, 1 cm. (c-d) The grain length and width were analyzed in transgenic lines and WT plants; n = 10 biologically independent plants per line were used for grain length analysis, n = 12 biologically independent plants per line were used for grain width analysis. In box plots, the line represents the median, the edges of the box define the interquartile range, and the whiskers represent the minimum and maximum values. Statistical significance was determined by a two-tailed Student's t test (*p < 0.05, **p < 0.01, ***p < 0.001). If pairwise comparisons of each of the three lines against the control yield P-values < 0.001, the figure reports the overall P-value obtained from a combined statistical test comparing the pooled experimental group (i.e., all three lines) with the control group.

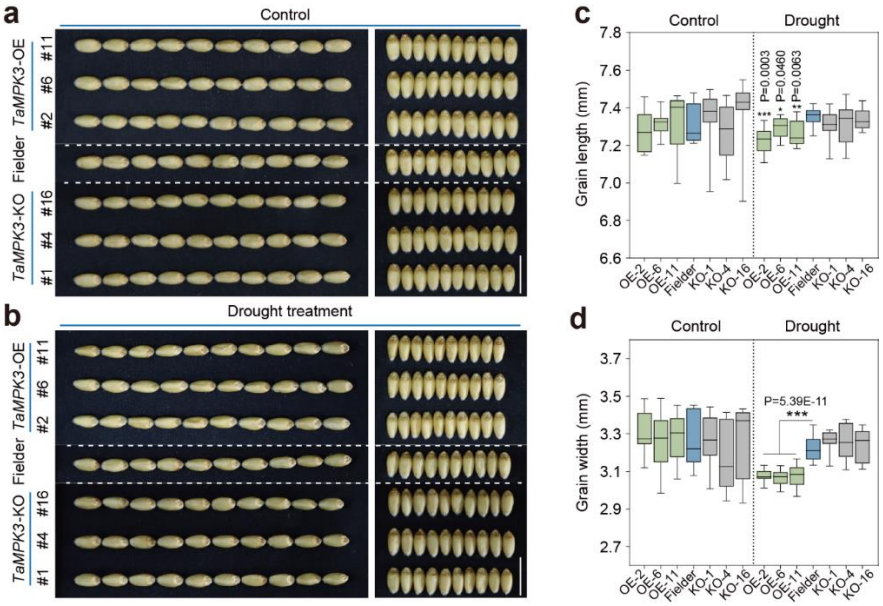

Supplementary Figure 8. Detection the influence of different concentrations of wheat extracts on the mycelial growth of *Fpg*. (a) *Fpg* colony growth on potato dextrose agar (PDA) medium containing different concentrations of wheat extracts; bars, 2 cm. (b) *Fpg* colony diameters calculated on medium with different concentrations of wheat extracts; n = 3 biologically independent colony per line. Data are presented as mean values +/- SD.

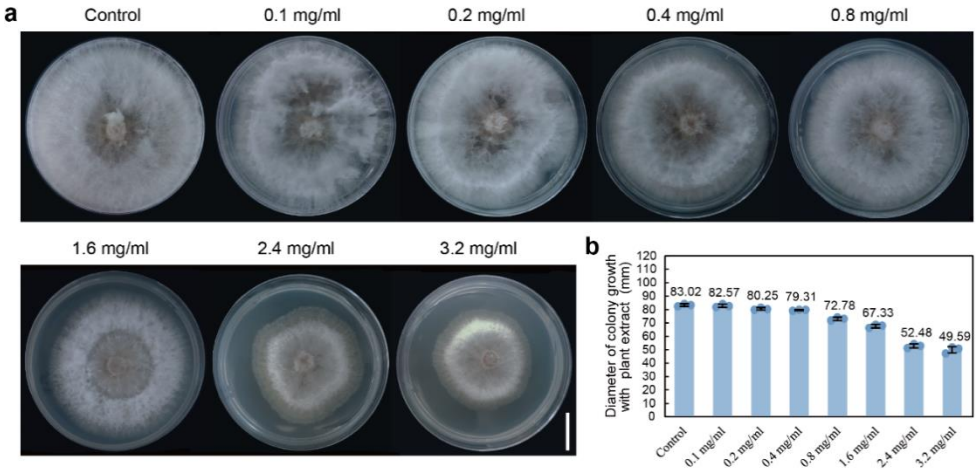

Supplementary Figure 9. Expression levels of sterol synthesis genes in stem bases of plants infected with *Fpg*. Data are presented as mean values +/- SD. Statistical significance was determined by a two-tailed Student's t test (***p < 0.001).

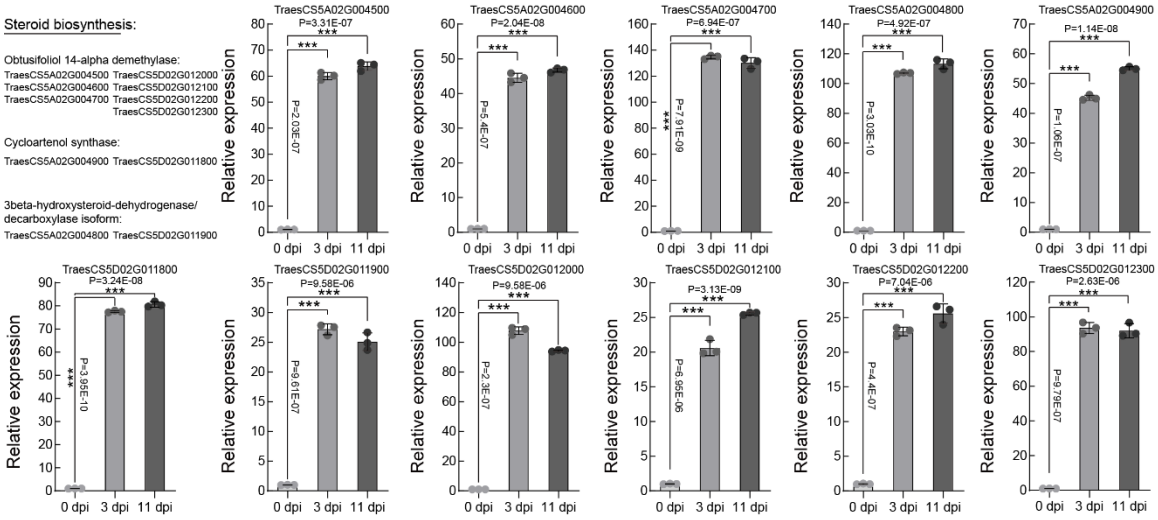

Supplementary Figure 10. Analysis of TaCYP51H37 protein abundance in *TaCYP51H37* overexpression lines (*TaCYP51H37*-OE) and WT plants.

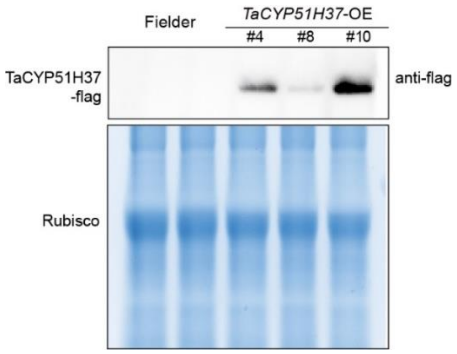

Supplementary Figure 11. The function of the *TaCYP51H37* gene in conferring *Fusarium* crown rot (FCR) resistance and drought tolerance was identified by virus-induced gene silencing (VIGS). (a) Phenotypes of BSMV: *TaCYP51H37* and control BSMV: γ plants grown under disease-free conditions and (b) *Fpg* infected condition; bars, 10 cm. (c-d and k) The expression of *TaCYP51H37* gene was detected in BSMV: *TaCYP51H37* lines and control plants. (e) Statistical analysis of the FCR disease indices in infected BSMV: *TaCYP51H37* and control plants. (f-h) The Shoot length, fresh weight and dry weight of BSMV: *TaCYP51H37* and control plants grown under normal and FCR infection conditions. (i-j) The drought resistance was analyzed in BSMV: *TaCYP51H37* and control BSMV: γ plants; bars, 10 cm. (l-m) The dry weight and MDA contents in BSMV: *TaCYP51H37* and control BSMV: γ plants grown under water-deficit conditions. Statistical significance was determined by a two-tailed Student's t test (*p < 0.05, **p < 0.01, ***p < 0.001). If pairwise comparisons of each of the three lines against the control yield P-values < 0.001, the figure reports the overall P-value obtained from a combined statistical test comparing the pooled experimental group (i.e., all three lines) with the control group. n = biologically independent plants.

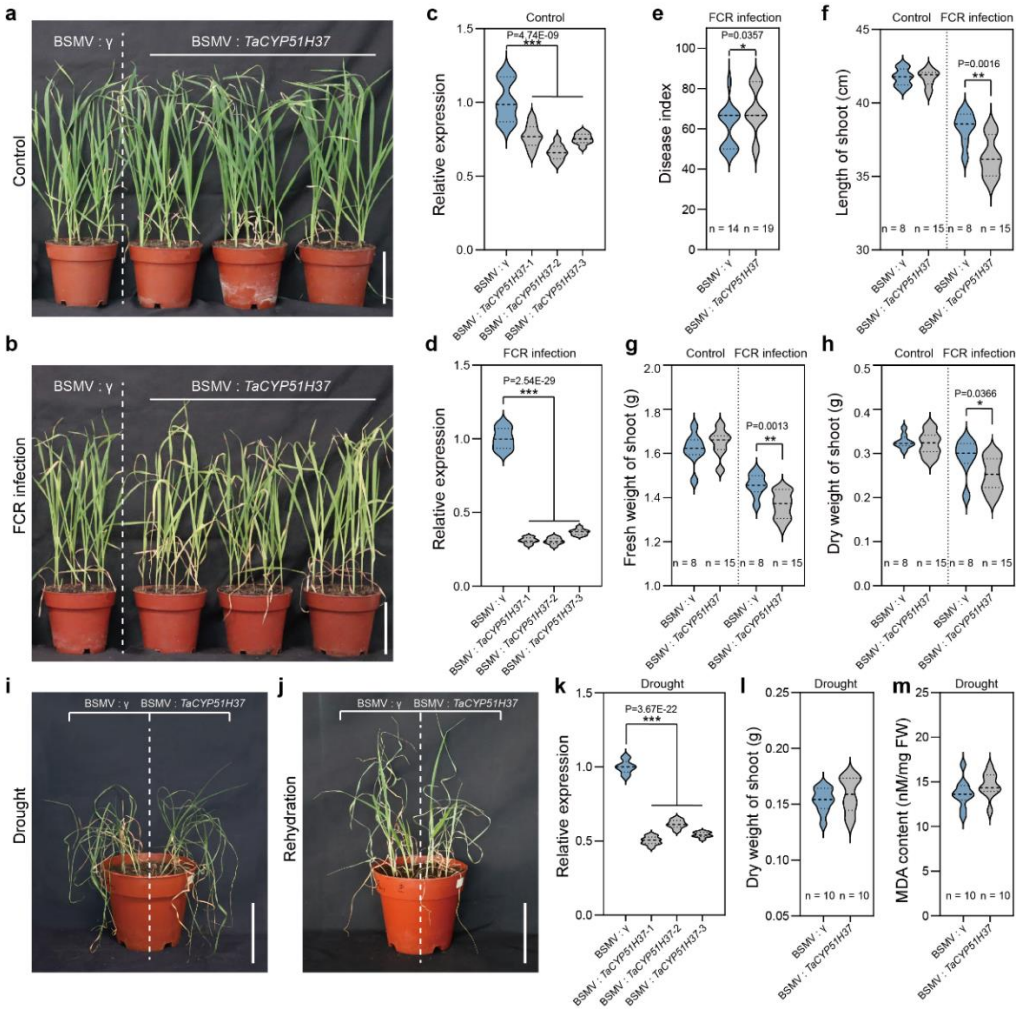

Supplementary Figure 12. Wheat germ agglutinin (WGA) fluorescence staining of stem base tissues in *Fpg*-infected *TaCYP51H37*-OE lines and WT plants.

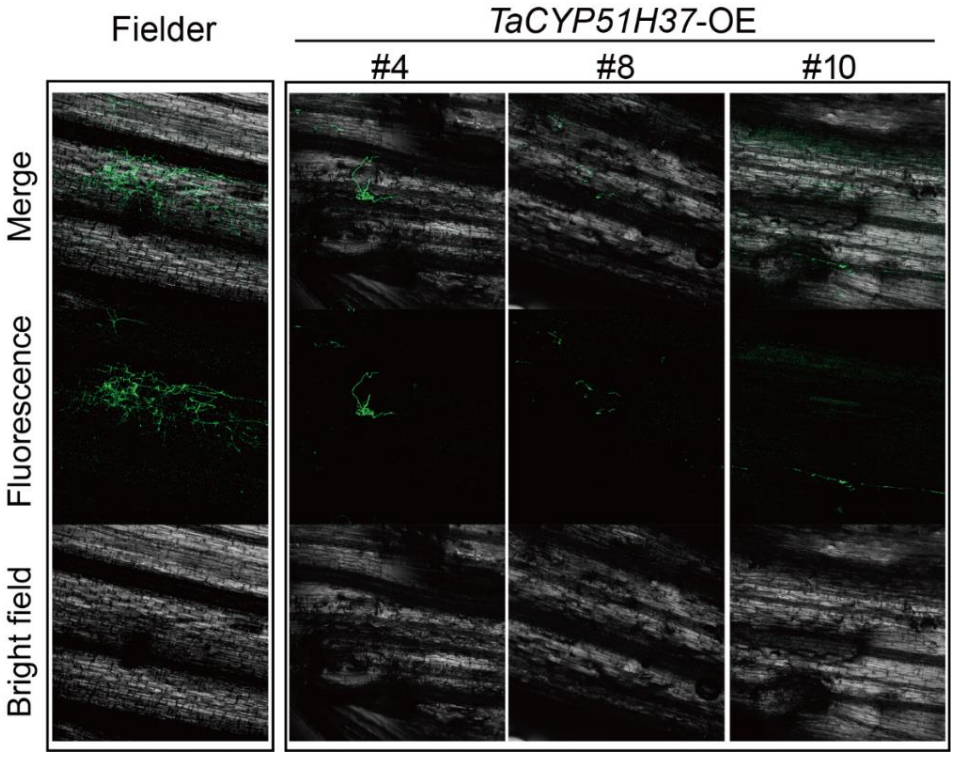

Supplementary Figure 13. Identification of drought resistance in *TaCYP51H37*-OE lines and the WT plants at seeding stage and adult stage. (a) Pheotypes of *TaCYP51H37*-OE and WT seedlings grown under water-deficit conditions; at 20 days post drought treatment (upper) and following 5 days of recovery (lower). (b-e) Dry weight, catalase (CAT), malondialdehyde (MDA), and proline (PRO) analyses of *TaCYP51H37*-OE and WT plants grown under water-deficit conditions; n = 12 biologically independent plants per line were used for dry weight analysis, n = 5 biologically independent plants per line were used for CAT activity and MDA contents analysis and n = 3 were used for PRO contents analysis. Data are presented as mean values +/- SD. (f) Phenotypes of *TaCYP51H37*-OE and WT lines grown under normal and drought conditions in the field. (g) The grains traits of *TaCYP51H37*-OE and WT lines. (h-m) Growth and yield traits of *TaCYP51H37*-OE and WT lines grown under normal and drought conditions in the field; n = 14 biologically independent plants per line were used for plant height and effective spike number analysis, n = 18 biologically independent plants per line were used for grain weight per plant and thousand grain weight analysis, n = 11 biologically independent plants per line were used for grain length and n = 12 were used for width analysis. In box plots, the line represents the median, the edges of the box define the interquartile range, and the whiskers represent the minimum and maximum values. Statistical significance was determined by a two-tailed Student's t test (*$p < 0.05$, **$p < 0.01$, ***$p < 0.001$). If pairwise comparisons of each of the three lines against the control yield P-values < 0.001, the figure

reports the overall P-value obtained from a combined statistical test comparing the pooled experimental group (i.e., all three lines) with the control group.

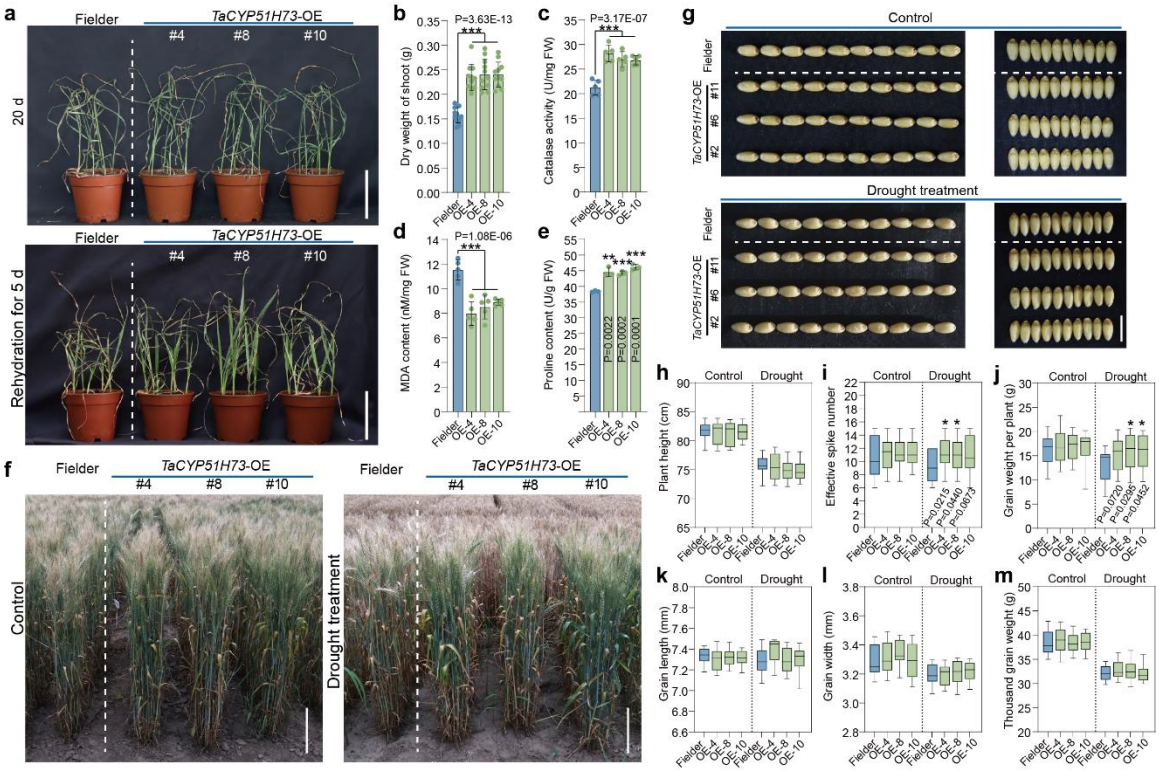

Supplementary Figure 14. Weighted gene co-expression network constructed using transcriptome data from wheat infected by *Fusarium pseudogramineum* and the transcriptome data of tissue expression. (a) Clustering of transcriptome data of each sample. Data with significant deviations, such as the data for first-leaf-blade-3, were excluded. (b) Module clustering of transcriptome data of each sample. The co-expression clustering of sterol synthesis genes was identified in the light purple module.

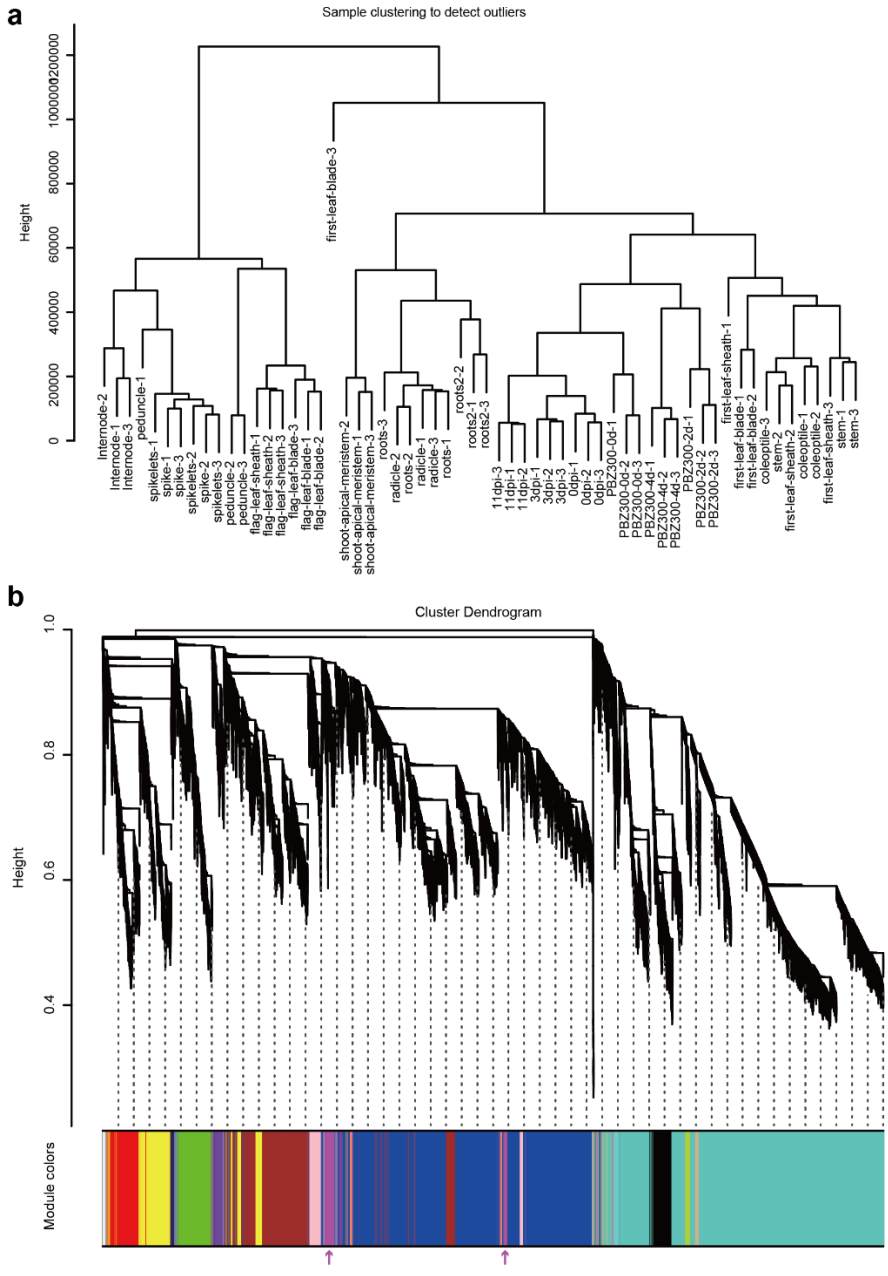

Supplementary Figure 15. The blank assay in the bimolecular fluorescence complementation (BiFC) system was employed to verify the absence of interaction between WRKY transcription factors and the empty cYFP vector.

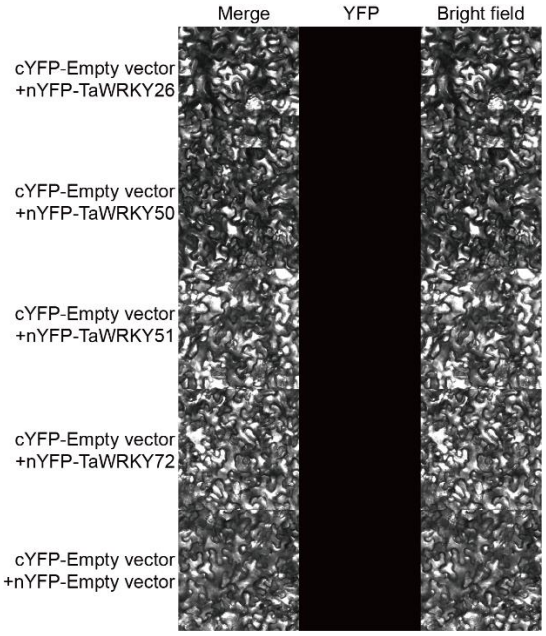

Supplementary Figure 16. Phos-tag assay was employed to identify the autophosphorylation of the TaMPK3 protein.

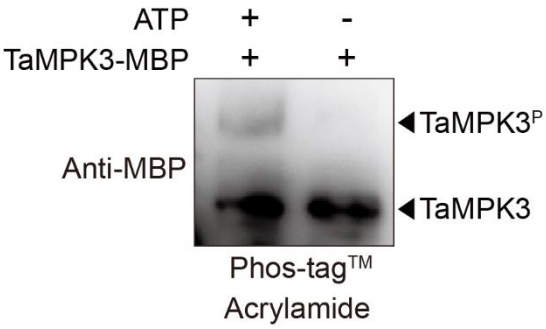

Supplementary Figure 17. The expression analysis of the *TaWRKY26* gene under *Fpg* inoculated (a) and drought treatment (b) in the stem base of wheat. Data are presented as mean values +/- SD. Statistical significance was determined by a two-tailed Student's t test (***p < 0.001).

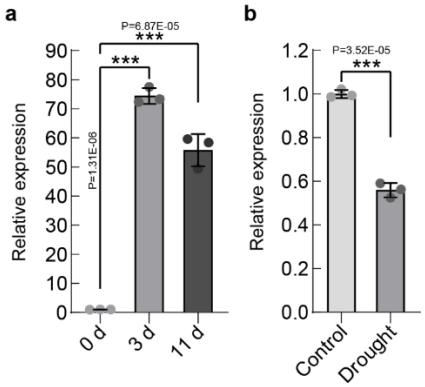

Supplementary Figure 18. The binding sites analysis of the WRKY transcription factor in the promoter regions of sterol synthesis genes.

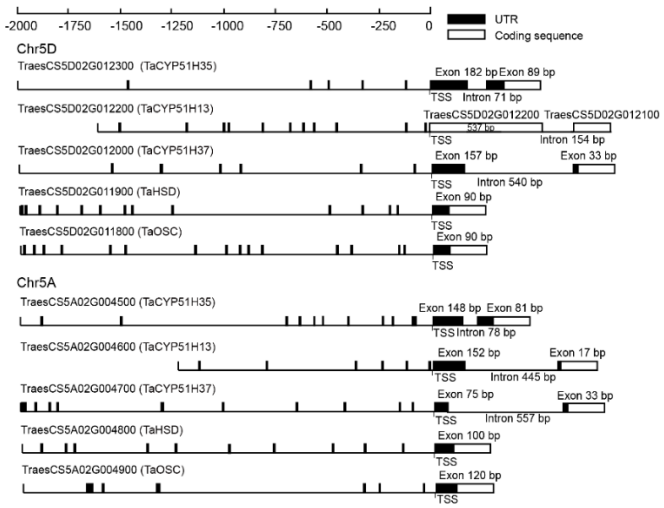

Supplementary Figure 19. Dual-luciferase reporter assay of sterol synthesis genes regulated by the TaMPK3 protein. OE, over expression.

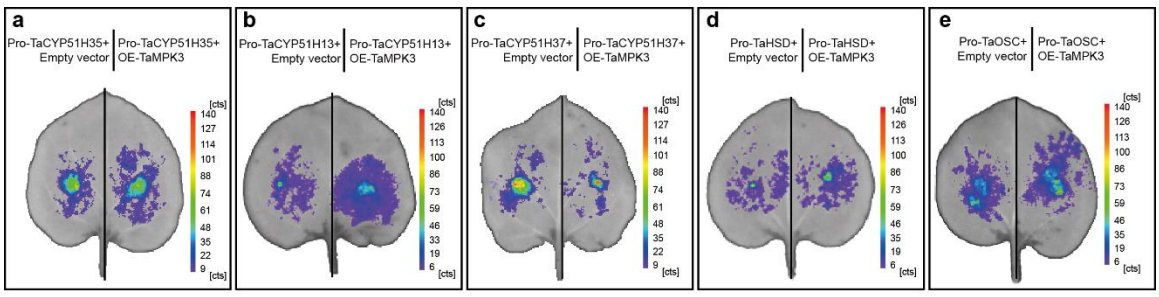

Supplementary Figure 20. Identification of FCR resistance conferred by the *TaWRKY26* gene using VIGS. (a) Phenotypes of BSMV: *TaWRKY26* plants and control BSMV: γ plants grown under normal and (b) FCR infected conditions; bars, 10 cm. (c-d and k) The expression of *TaWRKY26* gene was detected in BSMV: *TaWRKY26* lines and control plants. (e) Statistical analysis of the FCR disease indices in infected BSMV: *TaWRKY26* and control plants. (f-h) The shoot length, fresh weight and dry weight of BSMV: *TaWRKY26* and control plants grown under normal and FCR infection conditions. (i-j) The drought resistance was analyzed in BSMV: *TaWRKY26* and control BSMV: γ plants; bars, 10 cm. (l-m) The dry weight and MDA contents in BSMV: *TaWRKY26* and control plants grown under water-deficit conditions. Statistical significance was determined by a two-tailed Student's t test (*$p < 0.05$, **$p < 0.01$, ***$p < 0.001$). If pairwise comparisons of each of the three lines against the control yield P-values < 0.001, the figure reports the overall P-value obtained from a combined statistical test comparing the pooled experimental group (i.e., all three lines) with the control group. n = biologically independent plants.

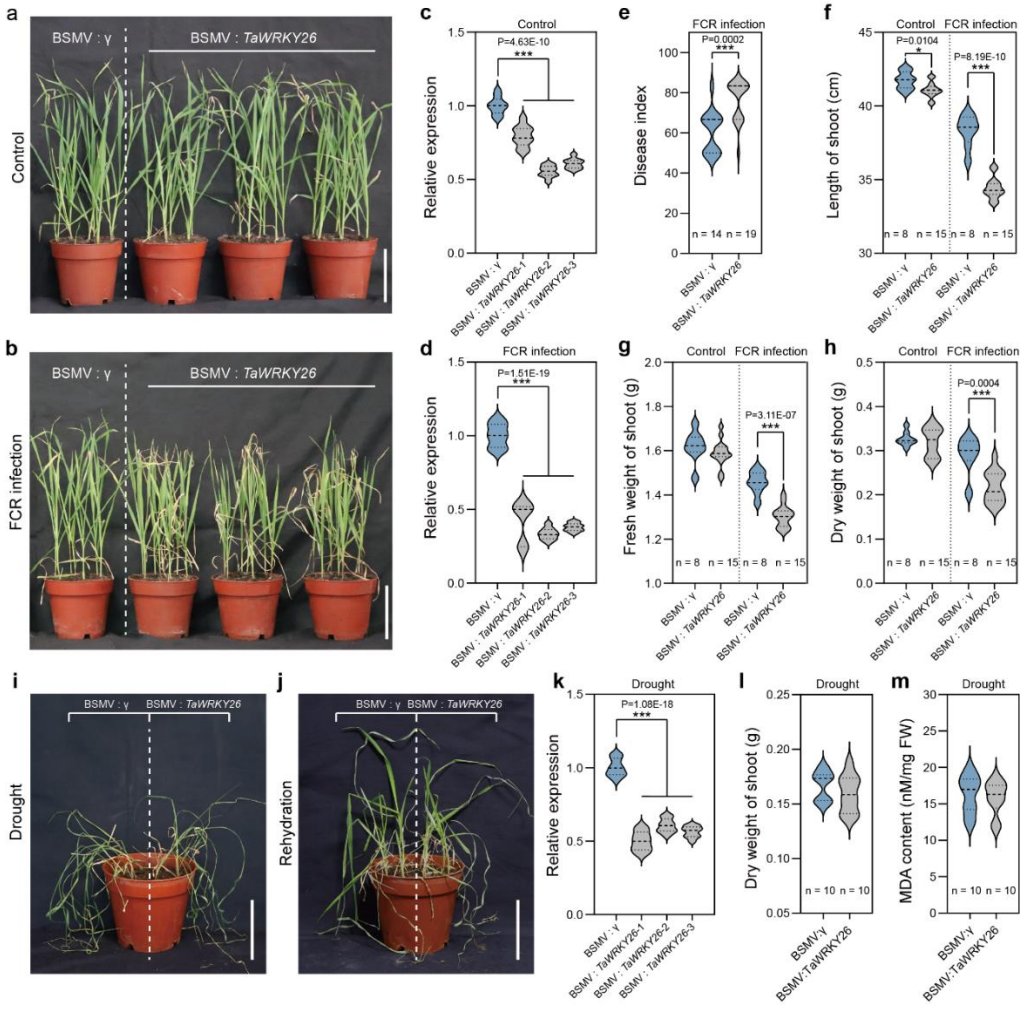

Supplementary Figure 21. The expression analysis of reported PYL protein downstream genes in wheat. (a) The expression analysis of reported PYL protein downstream genes in *TaMPK3*-OE, WT and *TaMPK3*-KO lines. (b) The expression analysis of reported FCR-related gene *TaCAT2* in *TaMPK3*-OE, WT and *TaMPK3*-KO lines. (c-d) The expression analysis of reported PYL protein downstream genes and *TaCAT2* in response to *Fpg* infection. (e) The expression analysis of reported PYL protein downstream genes in *TaCYP51H37*-OE lines and WT plants. (f) The expression analysis of reported PYL protein downstream genes in BSMV: *TaWRKY26* plants and control plants. In box plots, the line represents the median, the edges of the box define the interquartile range, and the whiskers represent the minimum and maximum values. Statistical significance was determined by a two-tailed Student's t test (*p < 0.05, **p < 0.01, ***p < 0.001). If pairwise comparisons of each of the three lines against the control yield P-values < 0.001, the figure reports the overall P-value obtained from a combined statistical test comparing the pooled experimental group (i.e., all three lines) with the control group.

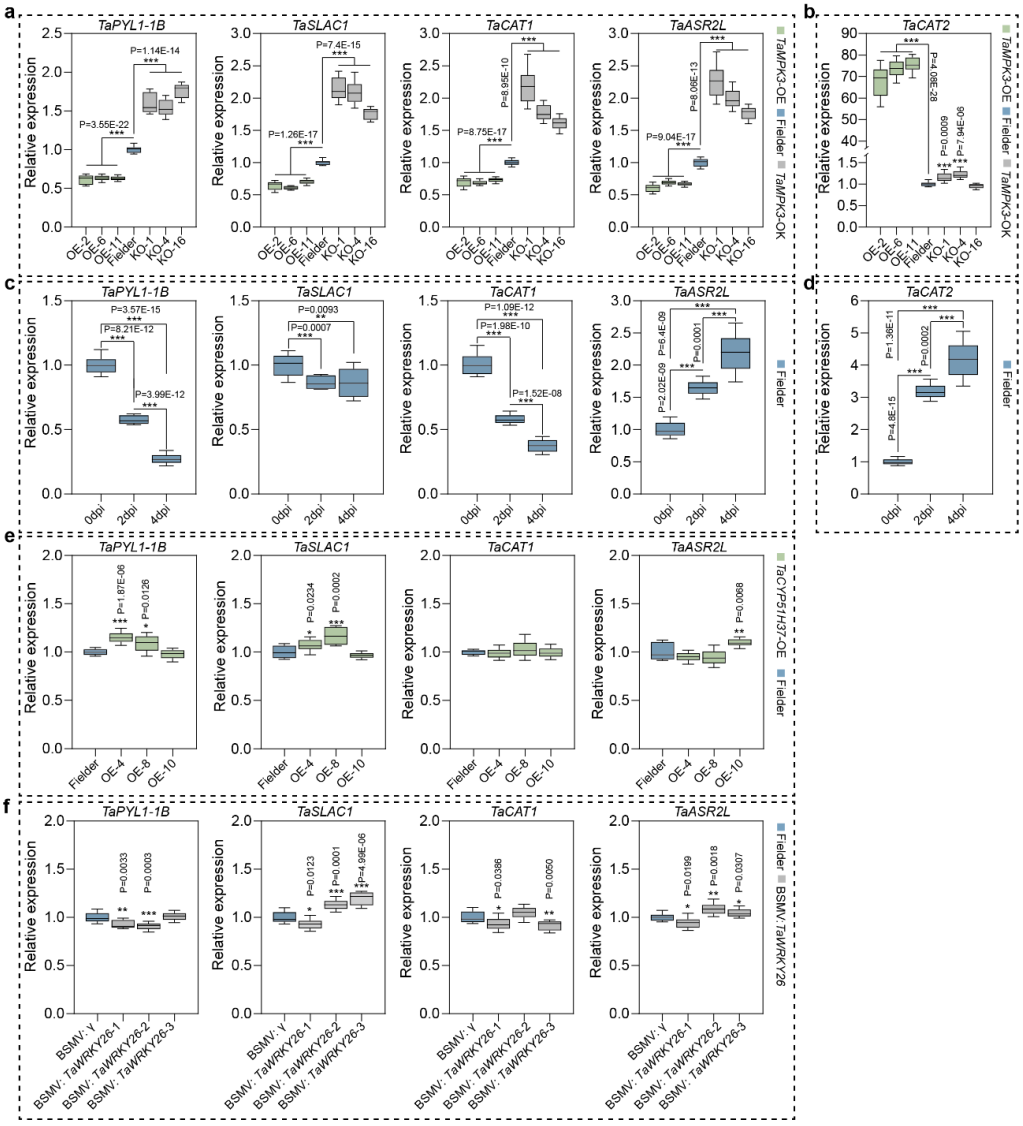

Supplementary Figure 22. Identification of FCR and drought resistance conferred by the *TaOSC* gene using VIGS. (a) Phenotypes analysis of BSMV: *TaOSC* lines and control BSMV: γ plants grown under normal condition or under (b) FCR and (c-d) drought stress; bars, 10 cm. (e) The FCR symptoms in BSMV: *TaOSC* lines and control plants; bars, 2 cm. (f) Statistical analysis of the FCR disease indices in infected BSMV: *TaOSC* lines and control plants, n = 10 biologically independent plants per line. (g-i) The dry weight of BSMV: *TaOSC* lines and control plants grown under normal condition or under FCR and drought stress, n = 10 biologically independent plants per line. (j) The MDA contents in BSMV: *TaOSC* lines and control plants grown under drought conditions, n = 10 biologically independent plants per line. (k-m) The expression of *TaOSC* gene was detected in BSMV: *TaOSC* plants and control plants. Statistical significance was determined by a two-tailed Student's t test (***p < 0.001). If pairwise comparisons of each of the three lines against the control yield P-values < 0.001, the figure reports the overall P-value obtained from a combined statistical test comparing the pooled experimental group (i.e., all three lines) with the control group.

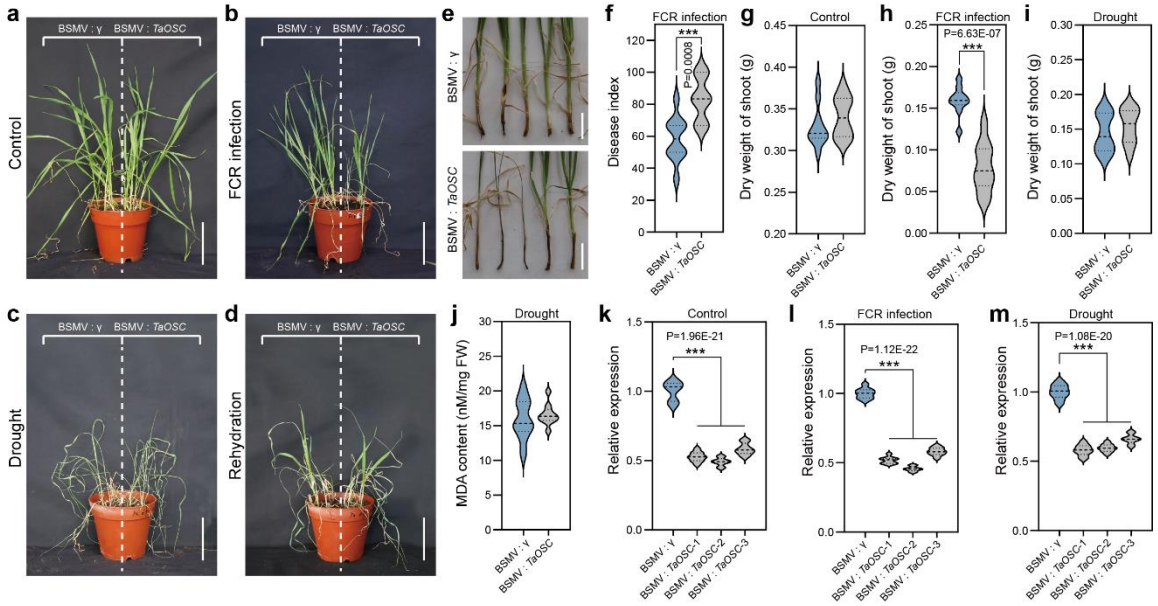

Supplementary Figure 23. Identification of FCR and drought resistance conferred by the *TaCYP51H35* gene using VIGS. (a) Phenotypes analysis of BSMV: *TaCYP51H35* lines and control BSMV: γ plants grown under normal condition or under (b) FCR and (c-d) drought stress; bars, 10 cm. (e) The FCR symptoms in BSMV: *TaCYP51H35* lines and control plants; bars, 2 cm. (f) Statistical analysis of the FCR disease indices in infected BSMV: *TaCYP51H35* lines and control plants, n = 10 biologically independent plants per line. (g-i) The dry weight of BSMV: *TaCYP51H35* lines and control plants grown under normal condition or under FCR and drought stress, n = 10 biologically independent plants per line. (j) The MDA contents in BSMV: *TaCYP51H35* lines and control plants under drought conditions, n = 10 biologically independent plants per line. (k-m) The expression

of *TaCYP51H35* gene was detected in BSMV: *TaCYP51H35* plants and control plants. Statistical significance was determined by a two-tailed Student's t test (*p < 0.05, **p < 0.01, ***p < 0.001). If pairwise comparisons of each of the three lines against the control yield P-values < 0.001, the figure reports the overall P-value obtained from a combined statistical test comparing the pooled experimental group (i.e., all three lines) with the control group.

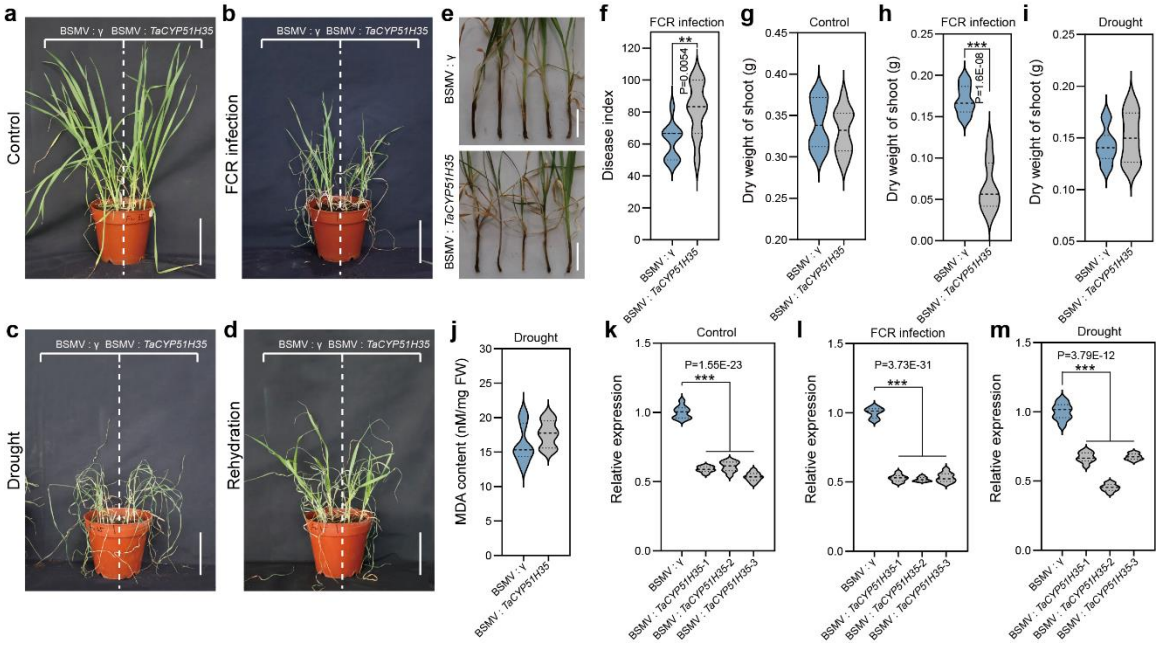

Supplementary Figure 24. Identification of FCR and drought resistance conferred by the *TaHSD* gene using VIGS. (a) Phenotypes analysis of BSMV: *TaHSD* lines and control BSMV: γ plants grown under normal condition or under (b) FCR and (c-d) drought stress; bars, 10 cm. (e) The FCR symptoms in BSMV: *TaHSD* lines and control plants; bars, 2 cm. (f) Statistical analysis of the FCR disease indices in infected BSMV: *TaHSD* lines and control plants, n = 10 biologically independent plants per line. (g-i) The dry weight of BSMV: *TaHSD* lines and control plants grown under normal condition or under FCR and drought stress, n = 10 biologically independent plants per line. (j) The MDA contents in BSMV: *TaHSD* lines and control plants grown under drought conditions, n = 10 biologically independent plants per line. (k-m) The expression of *TaHSD* gene was detected in BSMV: *TaHSD* plants and control plants. Statistical significance was determined by a two-tailed Student's t test (*p < 0.05, **p < 0.01, ***p < 0.001). If pairwise comparisons of each of the three lines against the control yield P-values < 0.001, the figure reports the overall P-value obtained from a combined statistical test comparing the pooled experimental group (i.e., all three lines) with the control group.

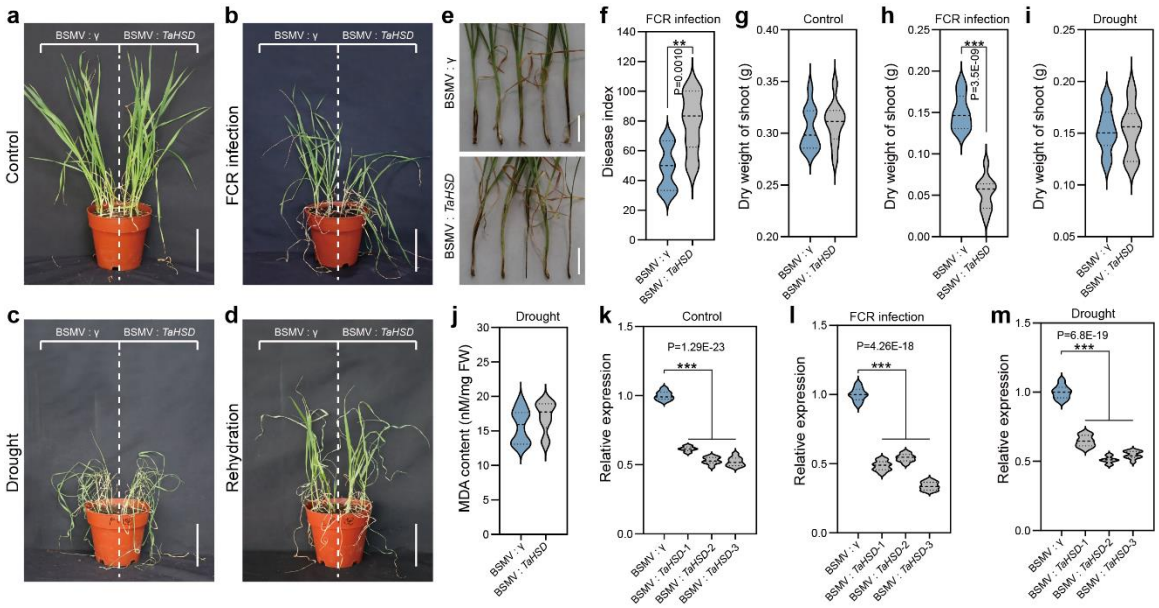
a
b
e
f
g
h
i
BSMV : γ
BSMV : TaHSD
Control
FCR infection
BSMV : γ
BSMV : TaHSD
Disease index
P=0.0010
**
Control
Dry weight of shoot (g)
FCR infection
P=3.5E-09
***
Drought
Dry weight of shoot (g)
c
d
j
k
l
m
Drought
Rehydration
Drought
MDA content (nM/mg FW)
Control
P=1.29E-23
***
FCR infection
P=4.26E-18
***
Drought
P=6.8E-19
***
Relative expression
BSMV : γ
BSMV : TaHSD-1
BSMV : TaHSD-2
BSMV : TaHSD-3

Supplementary Figure 25. Identification of drought resistance conferred by the *TaCYP51H37* and *TaMPK3* genes using VIGS. (a) Phenotypes of *TaCYP51H37* gene silencing in *TaMPK3*-OE lines under normal and (b-c) drought stress conditions; bars, 10 cm. (d-e) The expression of *TaCYP51H37* gene was detected in BSMV: *TaCYP51H37* plants and control plants. (f) The dry weight of BSMV: *TaCYP51H37* and control plants under normal and drought stress conditions, n = 10 biologically independent plants per line. (g) The MDA contents in BSMV: *TaCYP51H37* and control plants grown under drought conditions, n = 10 biologically independent plants per line. (h) Phenotypes of *TaMPK3* gene silencing in *TaCYP51H37*-OE lines under normal and (i-j) drought stress conditions; bars, 10 cm. (k-l) The expression of *TaMPK3* gene was detected in BSMV: *TaMPK3* plants and control plants. (m) The dry weight of BSMV: *TaMPK3* and control plants under normal and drought stress conditions, n = 10 biologically independent plants per line. (n) The MDA contents in BSMV: *TaMPK3* and control plants grown under drought conditions. n = 10 biologically independent plants per line. Statistical significance was determined by a two-tailed Student's t test (***p < 0.001). If pairwise comparisons of each of the three lines against the control yield P-values < 0.001, the figure reports the overall P-value obtained from a combined statistical test comparing the pooled experimental group (i.e., all three lines) with the control group.

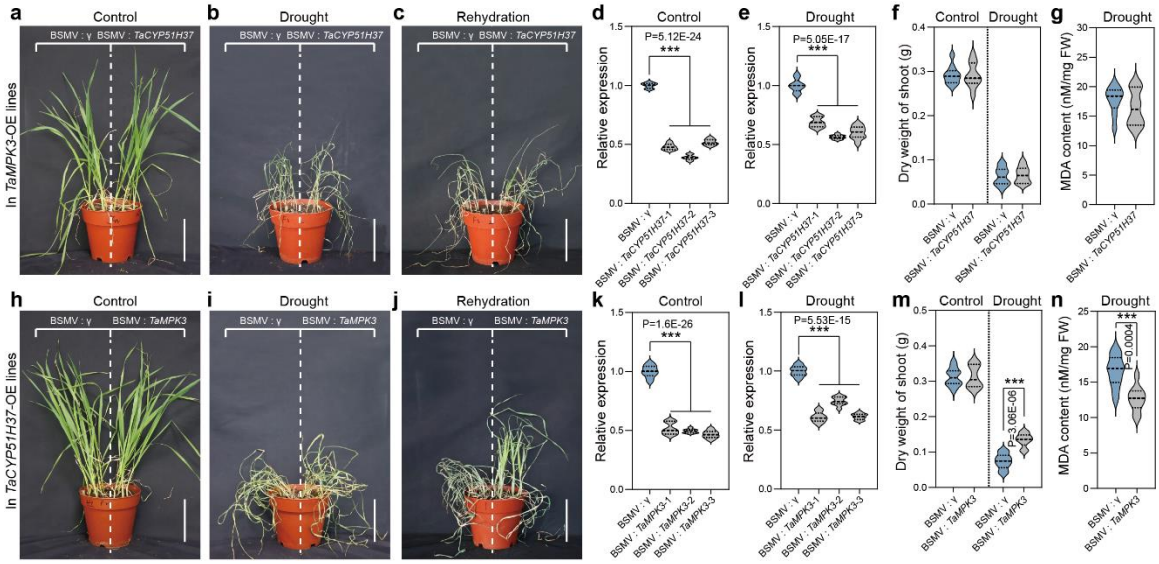

Supplementary Figure 26. SNP variation in the *TaMPK3* genes.

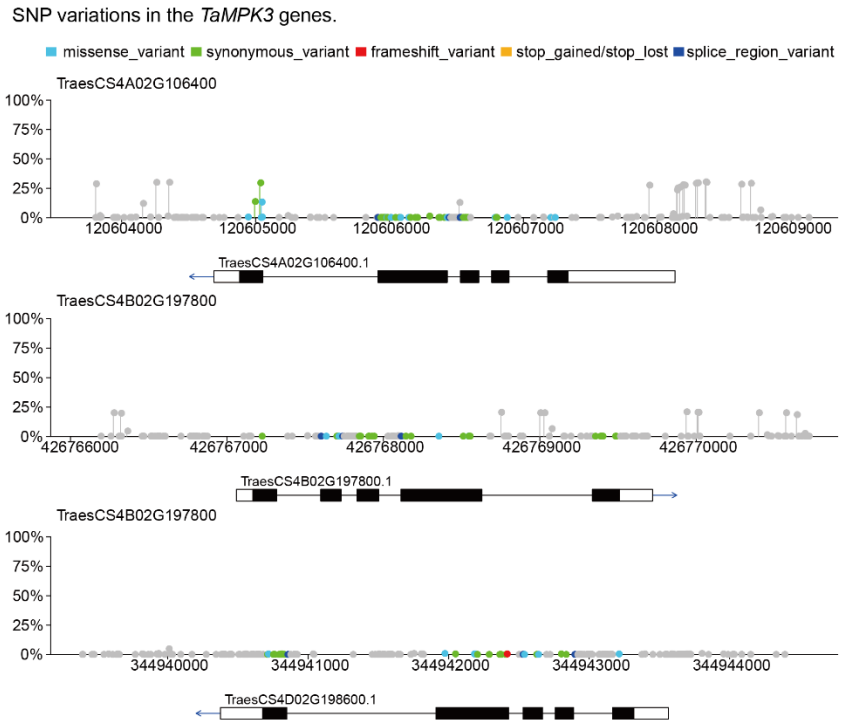

Supplementary Figure 27. SNP variations in the *TaWRKY26* genes.

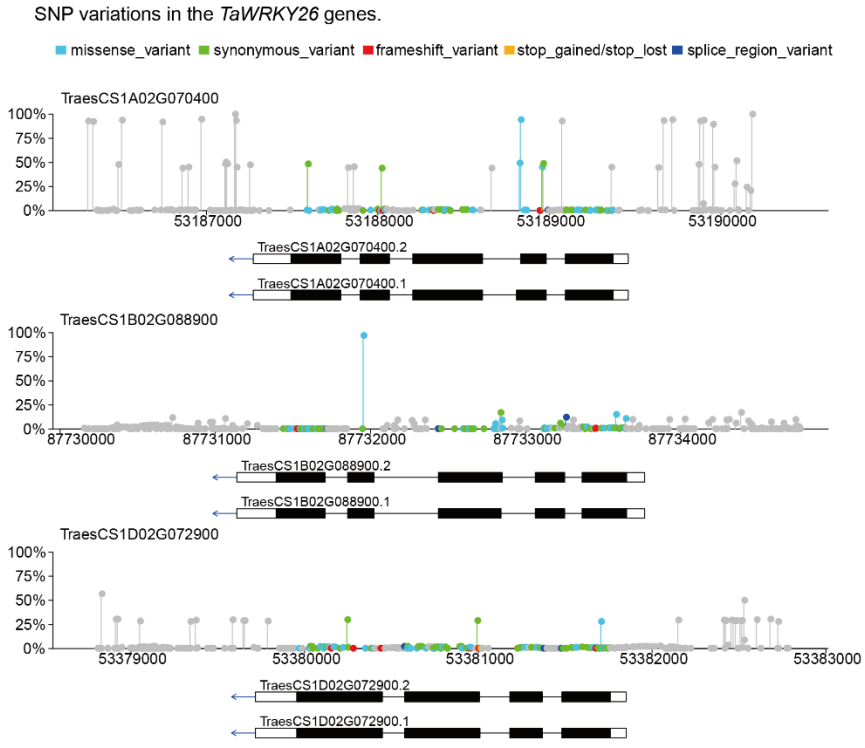

Supplementary Figure 28. Collinearity, gene structure, and WRKY transcription factor binding site analysis of sterol synthesis genes and their homologous genes. (a) Collinearity analysis of sterol synthesis genes and their homologous genes. (b) WRKY binding site analysis. (c) Gene structure analysis. (d) Expression levels of sterol biosynthesis-related genes and their orthologs in response to *Fpg* infection at 4 days post-inoculation. The sterol synthesis genes that responded to FCR infection are shown in reds. Data are presented as mean values +/- SD.

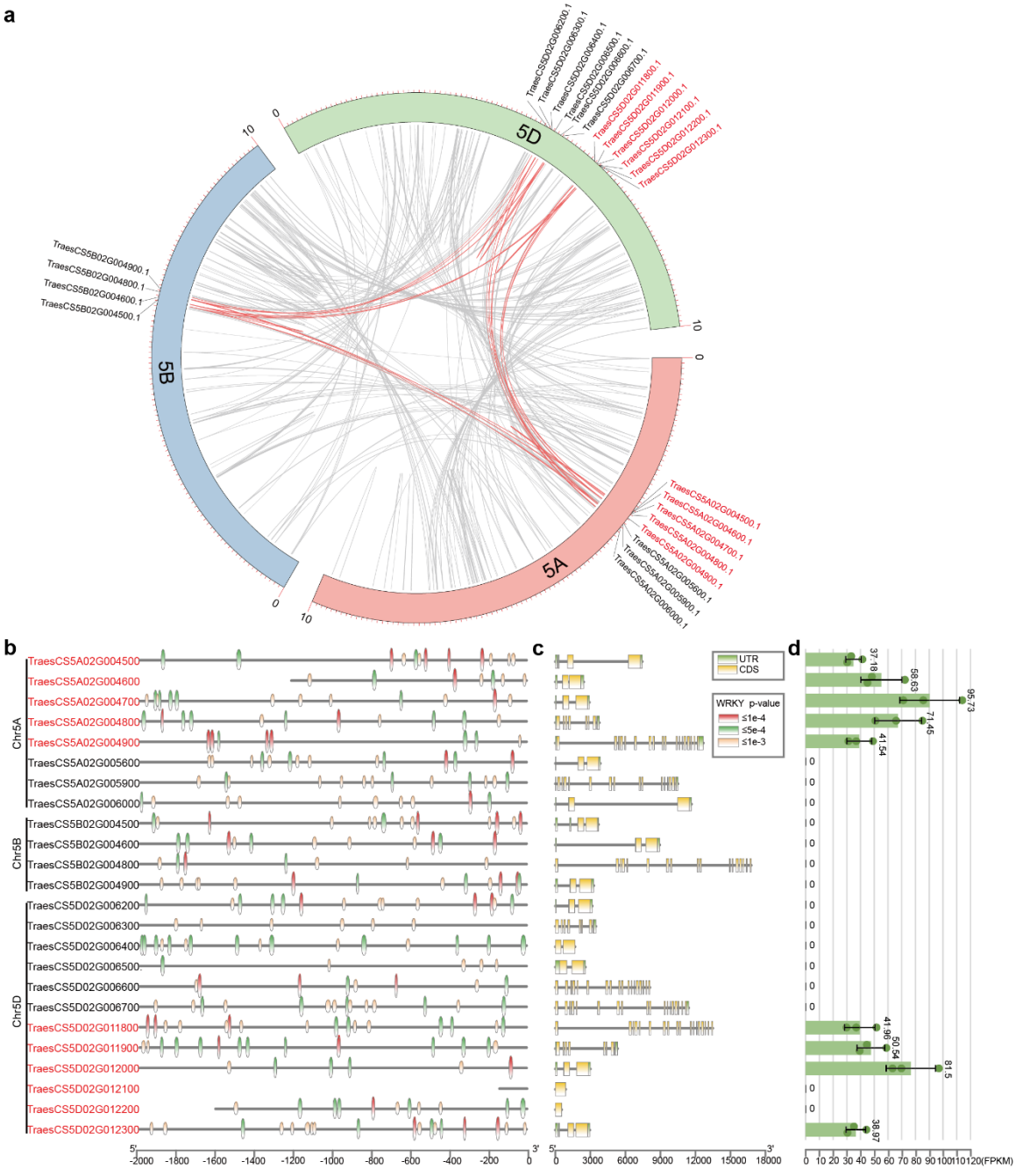

Supplementary Figure 29. SNP variations in sterol synthesis genes on chromosome 5A.

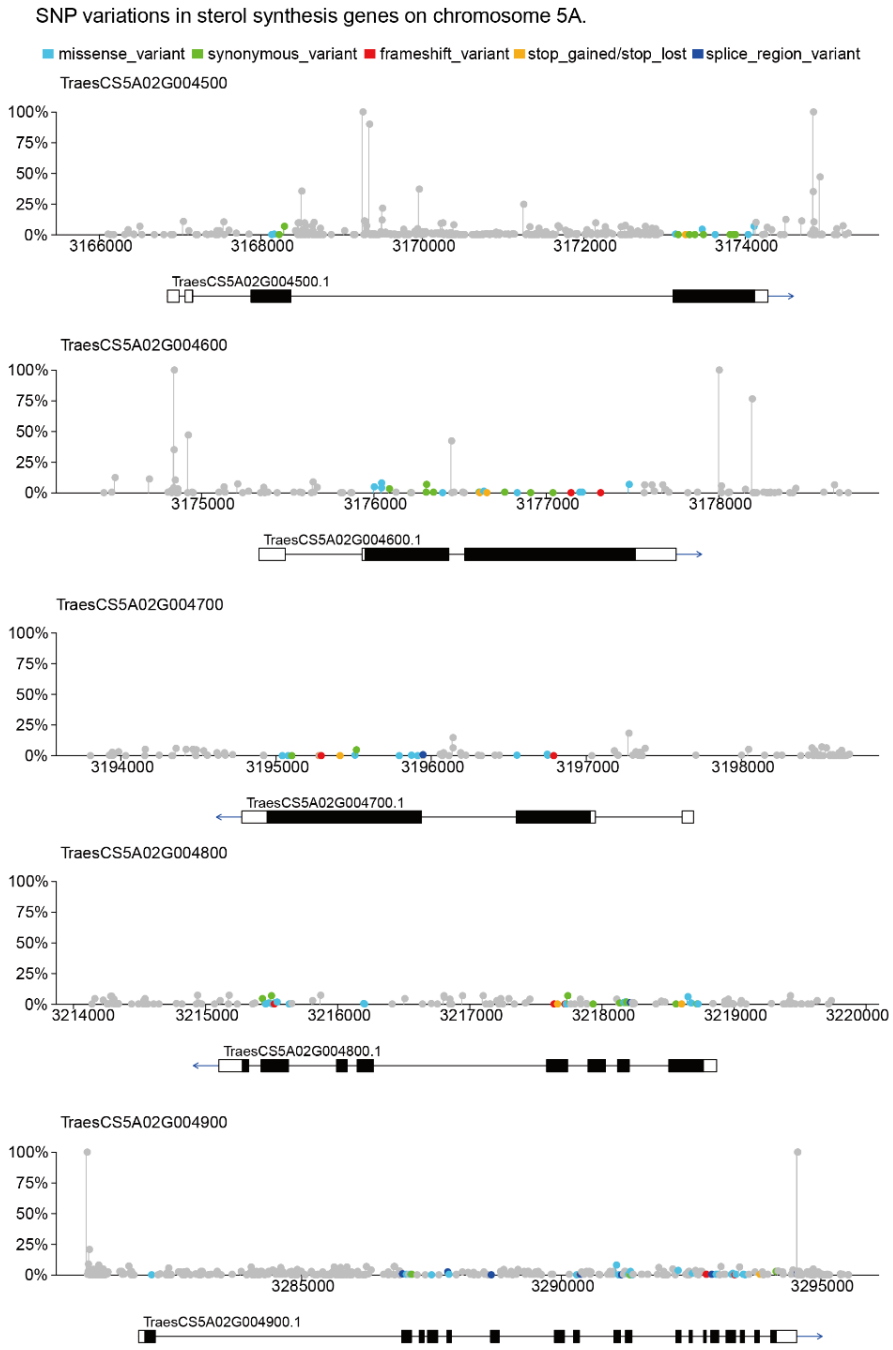

Supplementary Figure 30. SNP variations in sterol synthesis genes on chromosome 5D.

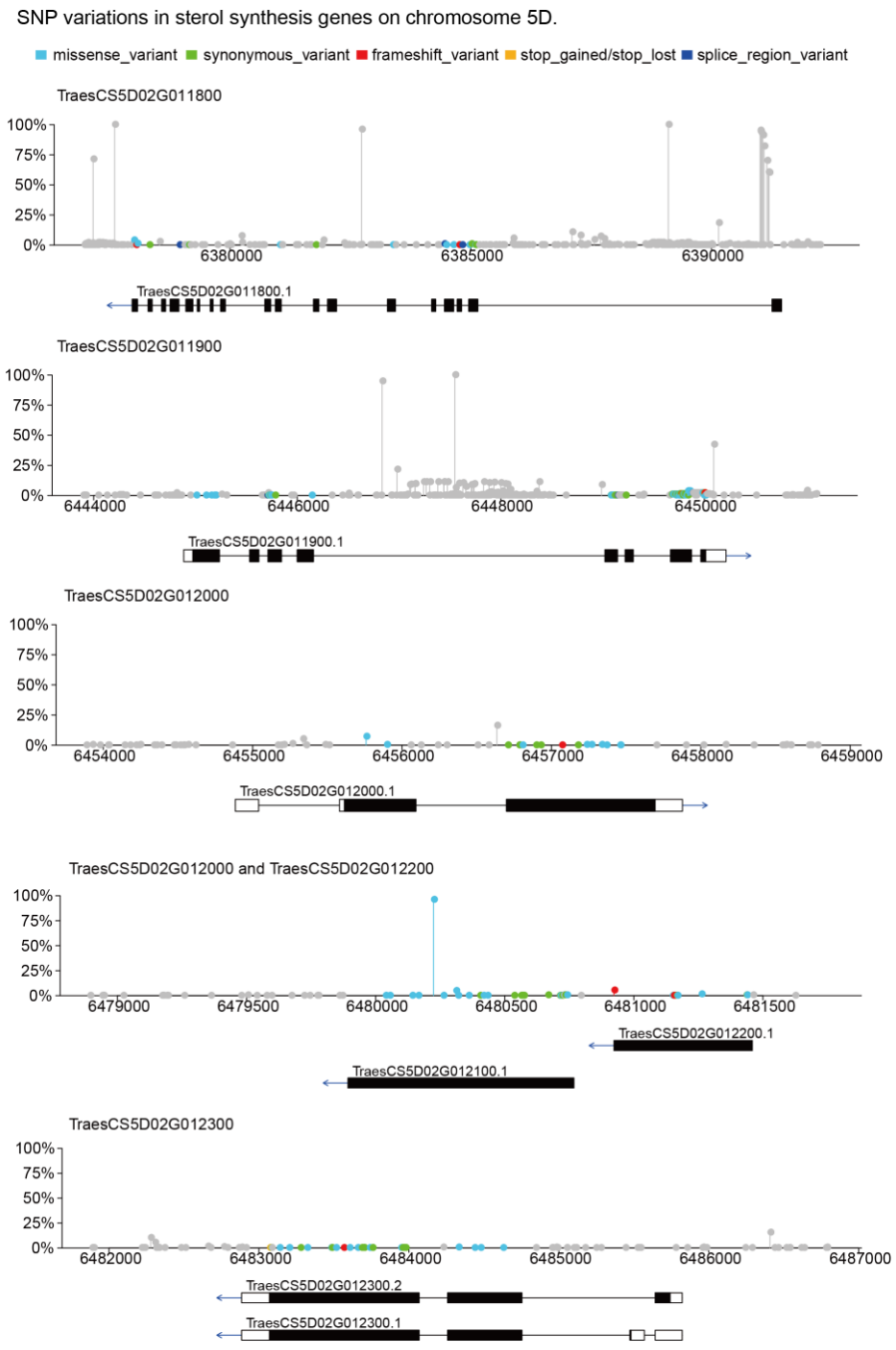

Supplementary Figure 31. SNP variations in homologous sterol synthesis genes on chromosome 5A.

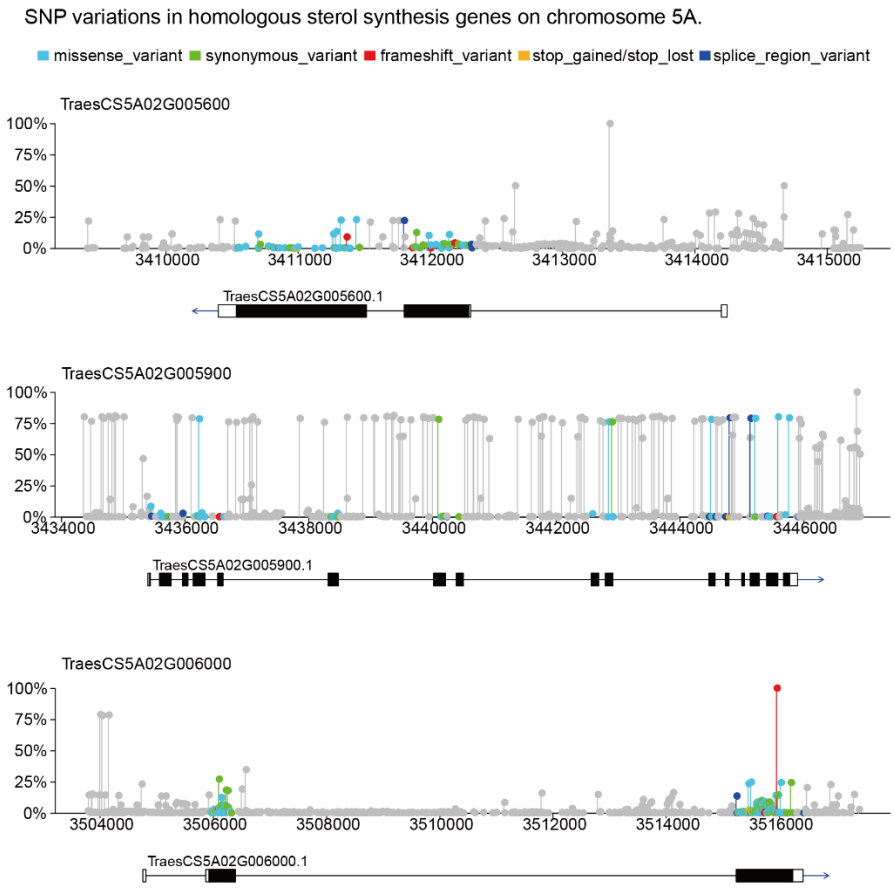

Supplementary Figure 32. SNP variations in homologous sterol synthesis genes on chromosome 5B.

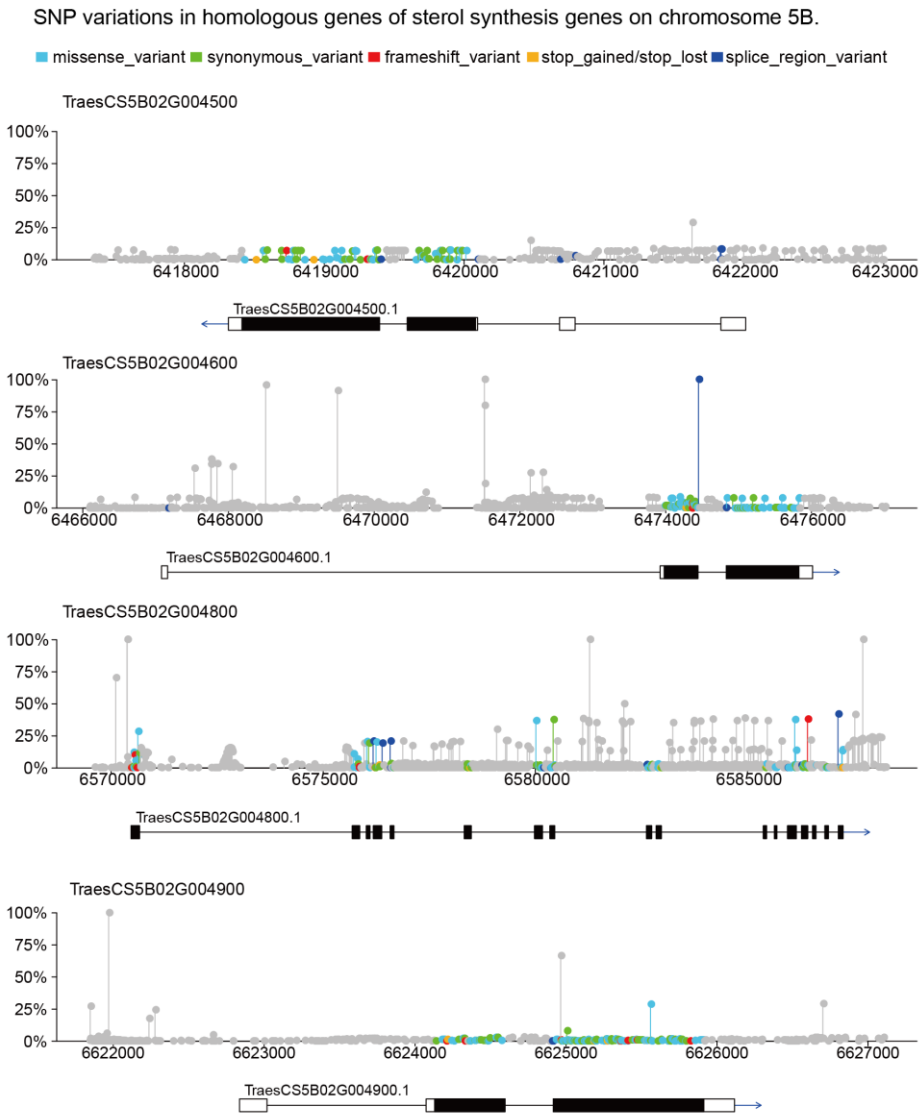

Supplementary Figure 33. SNP variations in homologous sterol synthesis genes on chromosome 5D.

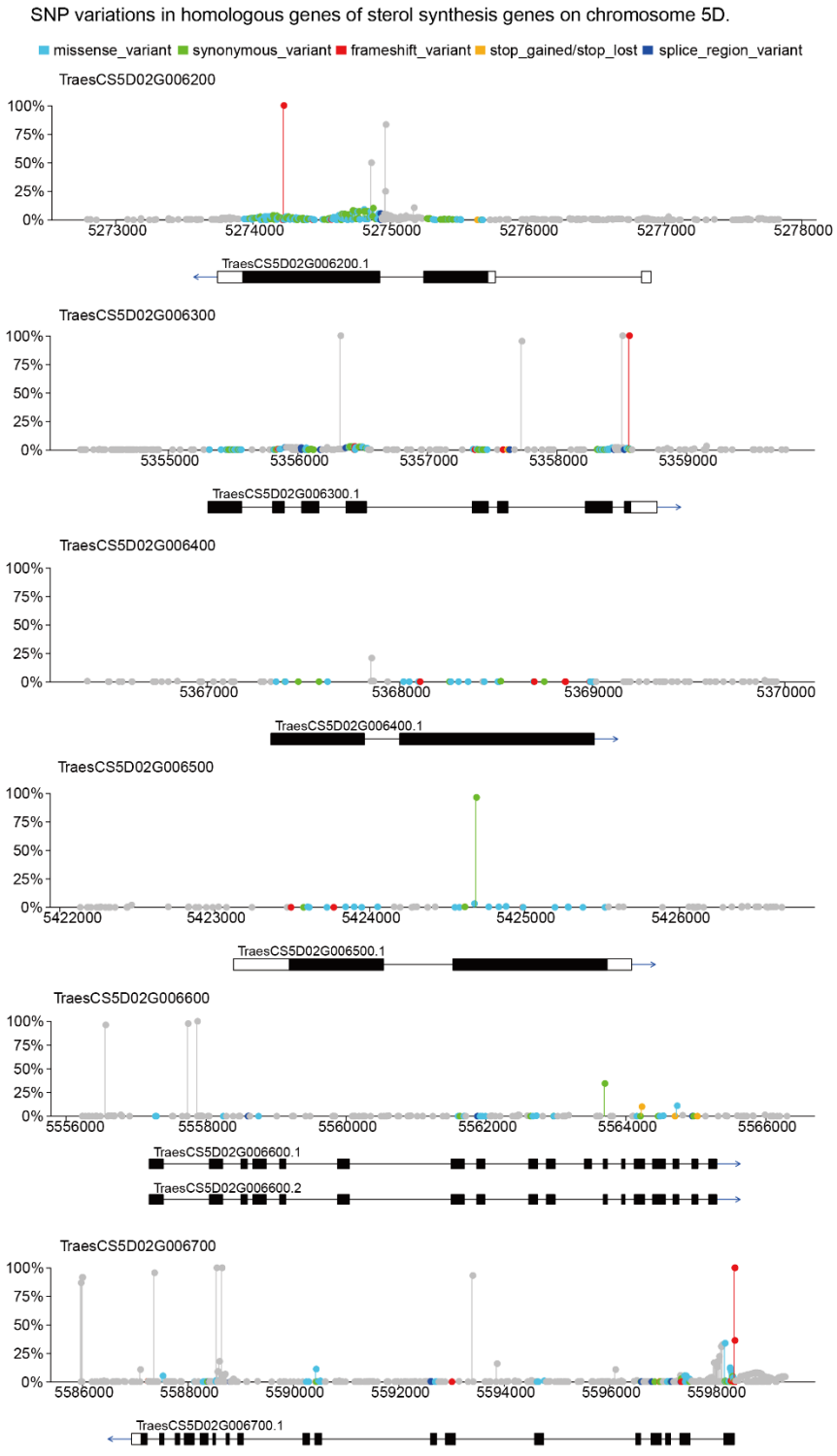

Supplementary Figure 34. Selection of VIGS target fragments and expression analysis of off-target genes. (a-e) Selection of VIGS target fragments of *TaWRKY26*, *TaCYP51H37*, *TaHSD*, *TaCYP51H35* and *TaOSC* genes. (f-g) The expression patterns of off-target gene were detected by RT-PCR. Statistical significance was determined by a two-tailed Student's t test (*p < 0.05, **p < 0.01, ***p < 0.001). (h) Analysis of the expression profiles of off-target genes within sterol biosynthesis gene clusters.